JOURNAL OF MATERIALS SCIENCE 27 (1992) 2606–2612

Application of scanning tunnelling microscopy to the study of fracture morphology of polycarbonate

C. M. AGRAWAL, K. HUNTER, G. W. PEARSALL, R. W. HENKENS
Department of Mechanical Engineering and Materials Science, Duke University, Durham, NC 27707, USA

Fracture tests were conducted on compact tension specimens of polycarbonate. The general morphology of the resulting fast, unstable fracture was analysed using optical and scanning electron microscopes. A technique was developed to enable the use of scanning tunnelling microscopy for studying the detailed fracture morphology of polycarbonate and other non-conducting materials. This technique yielded high-resolution pictures of the various regions on the fracture surface of polycarbonate. It also provided invaluable, quantitative descriptions of the step heights associated with the recesses, protrusions and other features on the fracture surface.

1. Introduction

A principal difference between the deformation behaviour and fracture of polymers compared to metals and inorganic glasses is the ability of polymers to craze. In tough glassy polymers like polycarbonate, crazes serve both as nucleation sites and precursors to cracks [1–8]. The energy associated with the formation of crazes accounts for a sizeable fraction of the total fracture energy [9, 10] and contributes toward the toughness of these engineering polymers. A promising approach to studying the micromechanics of crazing in polymers involves a detailed examination of the fracture morphology that results from craze-related deformation when a polymer is tested to failure under controlled conditions. Fast, unstable crack propagation through crazed material in polycarbonate results in the generation of characteristic patterns on the fracture surface, which have been the subject of several earlier studies [11–16].

Hull and Owen [12] identified four distinct areas on the fracture surface of polycarbonate.

1. Initiation region: crazes are the precursors to cracks [6, 17], and initially the crack grows by craze tearing [13, 18]. The initiation region has a very rough surface which shows evidence of ruptured craze fibrils and material "pull-out" [11]. Other studies [19, 20] have found vestiges of several crazes in this initiation region on post-fracture examination. The simultaneous development of crazes on different planes and their subsequent interaction can lead to a surface that has been characterized as a river pattern by Lee *et al.* [19]. Unstable crack growth initiates in one of these crazes [12].

2. Mist region: the mist region follows the initiation region and appears hazy to the naked eye. This region comprises "islands" of protruding and recessed material with the protrusions on each surface mating with the depressions on the other [12]. It is possible that this structure is the result of the crack oscillating between the two craze–matrix interfaces [13, 14]. Sometimes one or more sets of banded structures are superimposed on the "island" structure [20, 21].

3. Mirror region: this is an optically smooth region characterized by closed, elongated loops (roughly elliptical but elongated with major axis parallel to the direction of crack travel) called "conic" markings [11]. These markings are associated with a step change in the plane of crack propagation. It is difficult optically to resolve the height of this step. The interaction of the main crack with secondary cracks that initiate ahead of the main crack front on planes parallel but slightly removed from its plane presumably are responsible for these conic markings.

4. End band region: this is the fourth region on the fracture surface and is characterized by parallel, evenly spaced bands oriented perpendicular to the direction of crack propagation. Each band comprises two regions; the first region, closer to the fracture initiation site, shows evidence of pulled out material; the second region is relatively featureless and has a fine granular texture.

The features described above have been studied earlier using optical and scanning electron microscopy (SEM). However, because these microscopes depend on lens systems for focusing and magnification they are subject to aberrations inherent in these systems and are limited in resolution. This limitation makes it difficult to study the fine structure of the fracture morphology of fast fracture in polycarbonate, e.g. the step height of the conic markings and bands. The scanning tunnelling microscope (STM), on the other hand, does not use any lens systems and hence is able to give high lateral resolutions of the order of 0.2 nm [22]. An excellent introduction to the theory and

0022–2461

design of the STM has been provided by Hansma and Tersoff [23]. However, until now the STM has been used primarily for studying conducting materials like metals, semiconductors and graphite [24]. The present work was undertaken with the intent of adapting techniques for applying scanning tunnelling microscopy to the study of polymers which are generally non-conducting, and specifically, to use this technique to study the fracture morphology of polycarbonate.

2. Experimental procedure

2.1. Fracture tests and specimen preparation

The material used in this research was Lexan brand polycarbonate supplied in the form of extruded sheets of nominal thickness 12.7 mm. Compact tension specimens (CTS) were machined from these sheets as per specifications set out in ASTM standard E399-83. A technique described elsewhere [11, 25] was used to introduce the precrack in the CTS in order to avoid the heat generation and material orientation related problems associated with fatigue precracking in polymers. The fracture tests were performed in a tensile testing machine at a crosshead speed of 25.4 mm min^{-1}. Following the fracture test, an approximately 1 mm thick layer containing the fracture surface was removed from each specimen with a band saw. A low cutting speed was used to avoid overheating. The layer containing the fracture surface then was vacuum sputter-coated with approximately 20 nm of gold–palladium and examined using both scanning electron and scanning tunnelling microscopes.

2.2. Scanning tunnelling microscopy

The efficacy of applying a thin conductive film to poorly conducting substrates for imaging by a STM

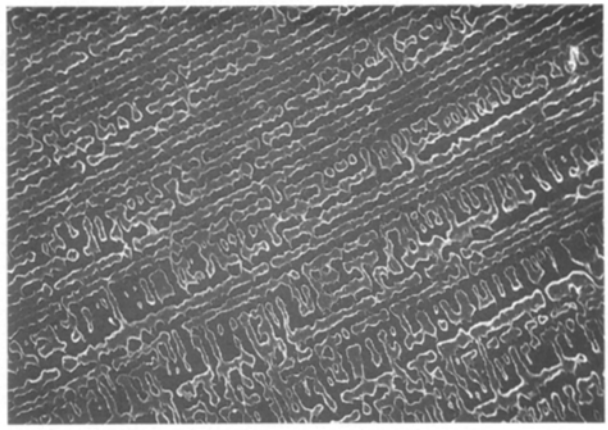

Figure 1 Transition in the mist region from island structure (lower right) to fine bands (upper left). Direction of crack travel: lower right to upper left corner (SEM fractograph, × 1500).

was demonstrated by Amrein *et al.* [26]. This method provides a means to examine the structure and morphology of polymer fracture surfaces.

The images and height profiles of the fracture surface obtained in this study were generated using a Digital Instruments Inc. Nanoscope II system, with a 9000 nm scanning head. Tunnelling tips were fabricated from polycrystalline tungsten wire of diameter 0.25 mm. A modification of the technique reported by Bryant *et al.* [27] was adopted to fashion sharp tips by the combined action of electrochemical etching and mechanical working.

The gold–palladium coated fracture surface was scanned at a tunnelling tip potential of + 80 to + 90 V. All scans were made in the "constant current" mode at a setpoint current of 2.20 nA. Acquired data were post-processed by a 3 × 3 digital convolution filter to remove high-frequency components from the image signal. These components carry little structural information and create an artificially "grainy" image for viewing. The topographic line plots were combined

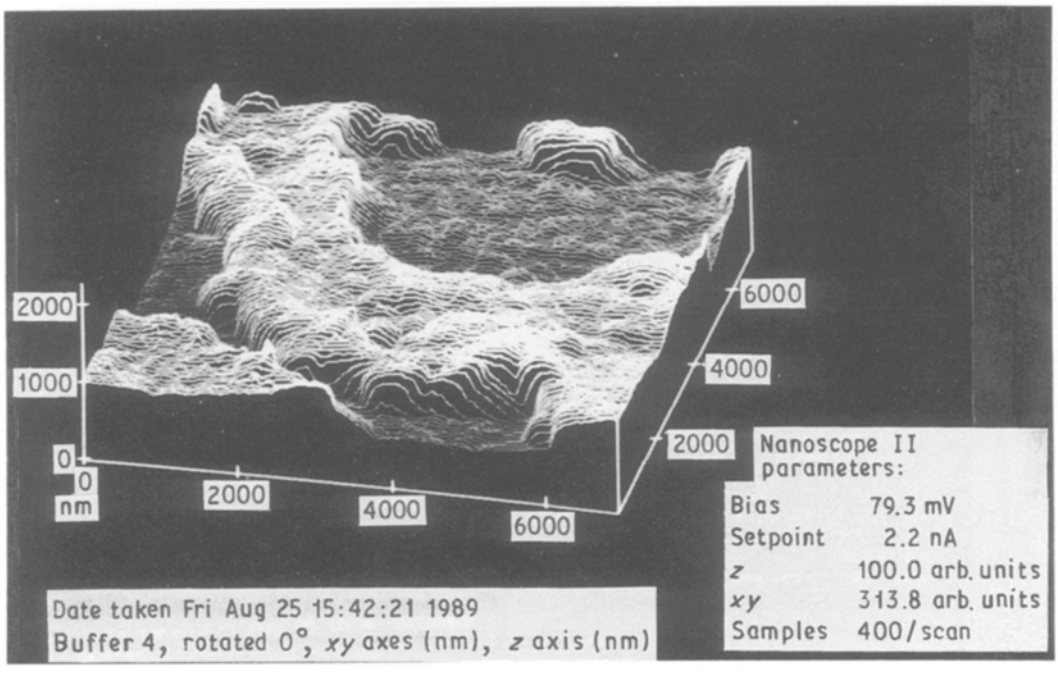

Figure 2 Mist region. Island with "lips" of material lining edges. Direction of crack travel: top to bottom of picture (STM fractograph).

with a grey scale imaging scheme which shows relative intensity as a function of height.

3. Results

The fracture surface of most specimens exhibited the same four distinct regions: an initiation region, a mist region, a mirror region with closed conic markings and an end band region, as described initially by Hull and Owen [12]. Post-fracture SEM examination confirmed that in the mist region protrusions on one fracture surface mate with recesses on the other and vice versa. The mist region comprised an island structure and a superimposed fine banded structure (Fig. 1).

TABLE I

Feature	Average step height (nm)
Islands with no "lips"	570
Islands with "lips"	460
Fine bands	360
Conic marking cavity	465
Conic marking protrusion	510

Upon examination in the STM at higher magnifications and resolutions, two different kinds of islands were identified: (i) islands with an average step height of approximately 460 nm (Table I) and a "lip" of

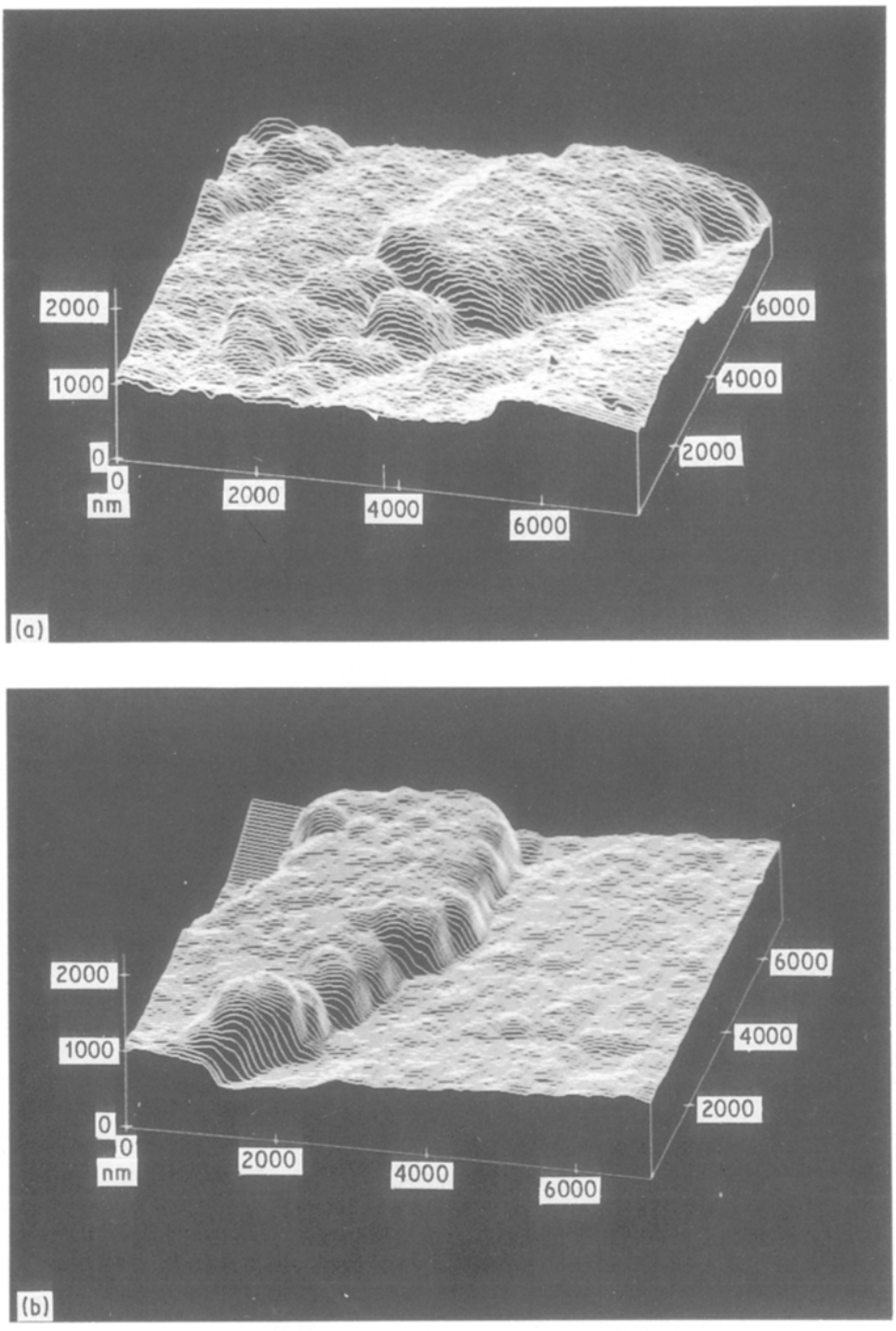

Figure 3 (a, b) Mist region. Islands without "lips". Average height of island structure = 570 nm. Direction of crack travel: (a) upper right to lower left corner, (b) top to bottom of picture; (STM fractographs).

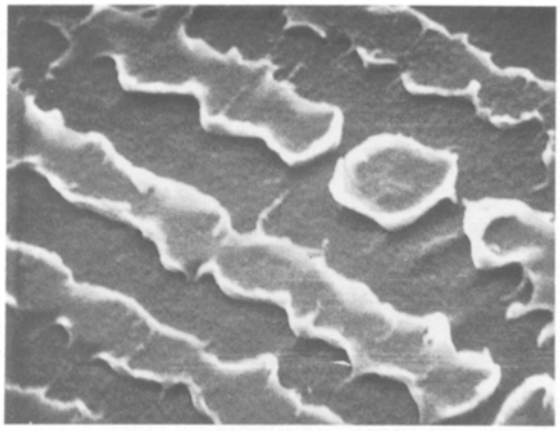

Figure 4 Fine bands in mist region with strips of crazed material along boundaries. Direction of crack travel: lower left to upper right corner (SEM fractograph, × 7000).

material on either side running parallel to the direction of crack propagation (Fig. 2). The average height of this lip measured from the protrusion was approximately 240 nm; (ii) islands that did not exhibit any lip structure but had an average height of approximately 570 nm (Fig. 3). The fine bands in the mist region also had lips of material on either side running parallel to the bands and perpendicular to the direction of crack propagation (Figs 4 and 5). The bands had an approximate height of 360 nm, and the lips were approximately 465 nm higher than the band protrusions. In both the bands and islands the top surface of the protrusions did not exhibit any significant substructure.

Evidence for both protruding and recessed conic markings was found in the mirror region. The recesses were approximately 465 nm deep (Table I) and had a lip of raised material along their edges (Figs 6–8). The average height of this lip was approximately 425 nm when measured from the plane of the main crack. However, on traversing the width of the conic section, the height of the raised lip was approximately 895 nm on one side of the conic marking and 1130 nm on the other when measured from the floor of the recess. Situated in the depression near the start of the conic marking there was found a hemispherical particle of diameter approximately 1145 nm and 70 nm high, relative to the floor of the depression (Fig. 7). The front of this particle was surrounded by a semi-circular channel (380 nm) recessed into the floor of the depression.

The protruding conic markings (Figs 9 and 10) had an average height of approximately 510 nm and at a few places had accompanying raised lips approximately 100 nm higher than the top surface. As in the case of the islands and the fine bands in the mist region, the top surfaces of these protrusions were fairly flat with no evidence of any significant substructure.

4. Discussion

4.1. Specimen preparation for microscopy

The technique developed in this study for preparing specimens by sputter coating with gold–palladium proved to be consistent and adequate for the purpose of fractography. This technique had an added advantage because the same specimens could be used for viewing by both STM and SEM. The 20 nm thick layer of gold–palladium sputter coated on the specimen surface was sufficiently thick to induce electrical conductivity and yet thin enough not to mask any significant morphological features. Because the specimens were approximately 1 mm thick they provided a stiff support to the fracture surface and eliminated the need for any special mounting.

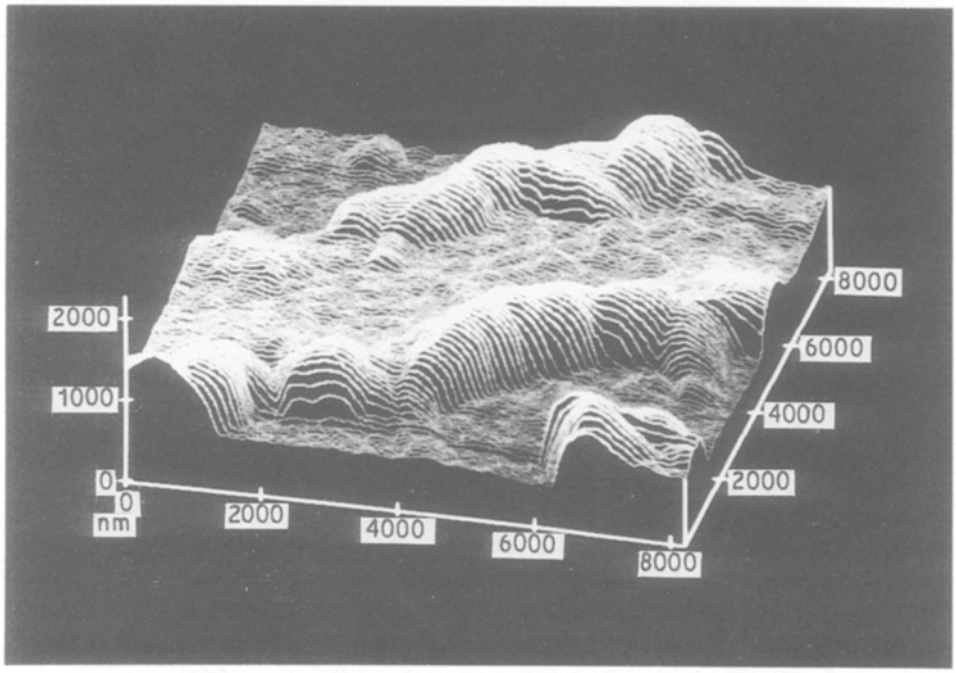

Figure 5 Fine band. Lips of material along boundaries suggest shear mode of failure. Direction of crack travel: lower right to upper left corner (STM fractograph).

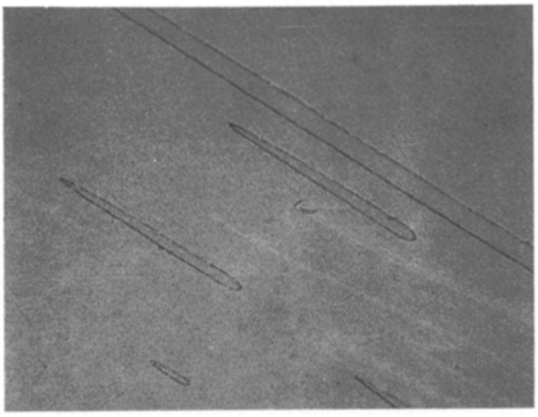

Figure 6 Conic markings in mirror region. Direction of crack travel: lower right to upper left corner (× 240).

4.2. Fracture morphology

4.2.1. Mist region

The mist region comprised an island structure and a region of fine bands. Both islands and fine bands exhibited lips of raised material along their edges. These lips suggest shear failure at these locations. In their work on polystyrene, Murray and Hull [21] proposed that the acute stress ahead of the crack tip causes decohesions and secondary cracks on the craze–matrix interface ahead of the main crack front. The results reported here suggest that the same mechanism probably governs the failure of polycarbonate in the mist region. As the main crack, propagating along one of the craze–matrix interfaces, approaches a decohesion on the other interface, the remaining ligament of polymeric material between the two cracks deforms and fails in shear. The deformed material then snaps back on to either interface giving rise to the lips lining the islands and fine bands. As the main crack encounters the decohesion-initiated secondary crack it changes its plane, and this change results in the formation of the mating protrusions and depressions on the two fracture surfaces.

4.2.2. Mirror region

The conic markings in the mirror region also exhibited lips of deformed material along their sides. Possibly the mechanism responsible for the generation of these lips is analogous to that described above for the mist region. However, previous work suggests that in the mirror region the crack follows the leading edge of the craze very closely, and hence the craze does not have sufficient time to grow in thickness [11]. It is possible that decohesion at the craze–matrix interface occurs only when the craze thickness is above some critical threshold which is higher than the craze thickness in the mirror region. In the mirror region secondary cracks are initiated ahead of the main crack at impurities which might be in the form of inclusions. Conic markings would then be generated when the main crack overtakes those secondary cracks that are on planes parallel to, but slightly removed from, its own plane. This process is accompanied by a step change in the plane of the crack and the generation of lips. Based on the earlier work of Andrews [28], Agrawal and Pearsall [11] have shown that the conic markings are expected to be closed (elliptical instead of parabolic) when the velocity of the main crack is greater than that of the secondary crack and their relative velocity is decreasing.

On comparison of Figs 7 and 8 it can be seen that in the STM the lips of deformed material appear to be well rounded hillocks, while in the SEM these lips appear as flaps of material overhanging the cavity of the conic marking. A limitation of the STM is the inability of its tunnelling tip to follow closely a surface that is undercut. Hence, Fig. 8 should be considered

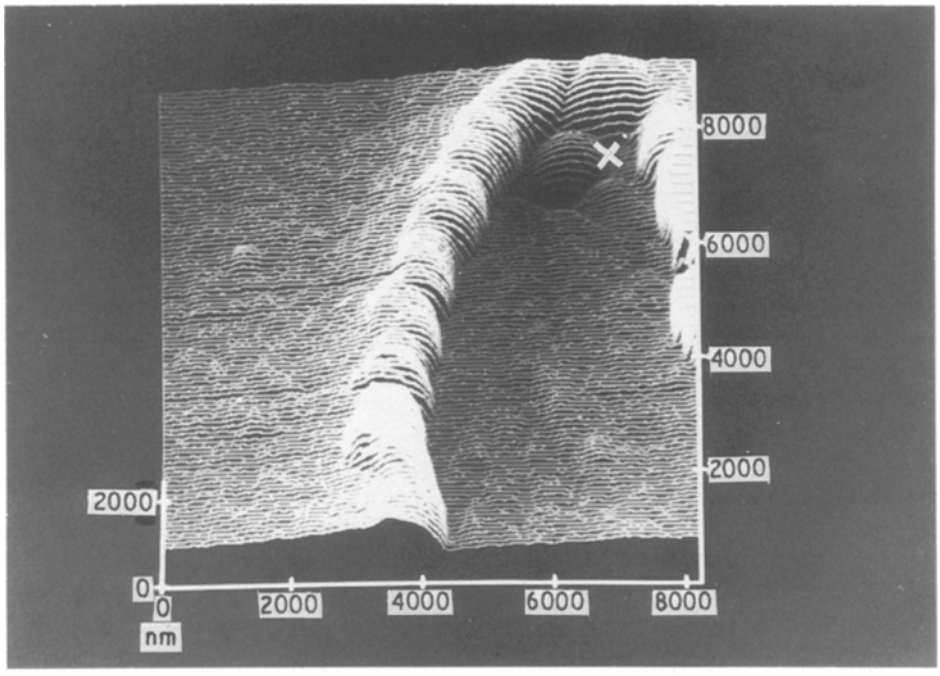

Figure 7 Portion of recessed conic marking showing "inclusion" (X) and lips of deformed material along boundaries. Direction of crack travel: top to bottom of picture (STM fractograph).

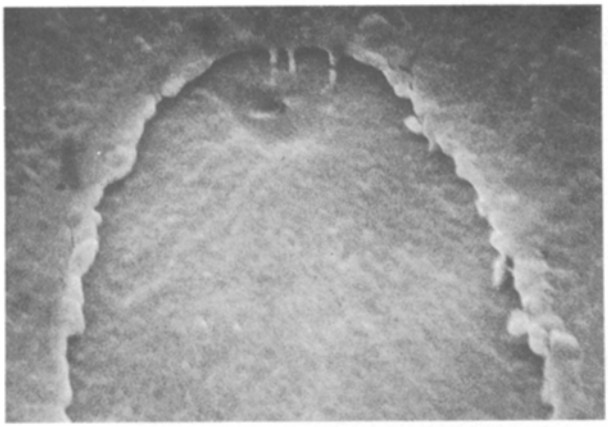

Figure 8 Part of recessed conic marking. Direction of crack travel: top to bottom of picture (SEM fractograph, × 10000).

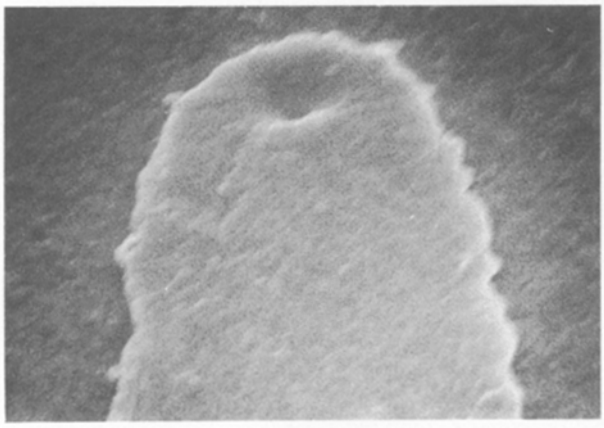

Figure 9 Portion of protruding conic marking. Direction of crack travel: top to bottom of picture (SEM fractograph, × 10000).

a more accurate representation of the raised lips of deformed material. However, the STM provides invaluable, quantitative information about the step heights associated with the lips, cavities and protrusions of the conic markings on the fracture surface. The average step heights of approximately 465 and 510 nm for the cavities and protrusions, respectively, measured in this study agree with the average step height of 500 nm measured by Hull and Owen [12] using optical techniques. Hull and Owen [12] also reported the presence of particles and voids at the focus of each conic marking. The results of the present study support these observations as shown in Figs 7–9. The precise nature of the particle shown in Fig. 7 has not been established. However, it is likely that it is an inclusion that was an inadvertent by-product of manufacturing process. It is also possible that its smooth well-rounded surface may have resulted in part from the gold–palladium coating applied to the fracture surface. The channel surrounding the particle may have been created by the polymer matrix detaching itself from the particle under the applied stress.

5. Conclusions

The technique developed in the present work to study the fracture surface of polymers using scanning tunnelling microscopy was successfully used to investigate the fast, unstable fracture of polycarbonate. This technique provided convenient and accurate measurements of the step heights and the dimensions of the various microscopic features on the fracture surface. The high-resolution microscopy provided by the STM showed the presence of raised lips of deformed material lining the islands, fine bands and the conic markings. These lips are interpreted as indicating failure by shear at these locations and give credence to the theory of decohesion at the craze–matrix interface ahead of the main crack as proposed by Murray and Hull [21].

In the mirror region, voids or particles are observed at the focus of each conic marking. It is possible that

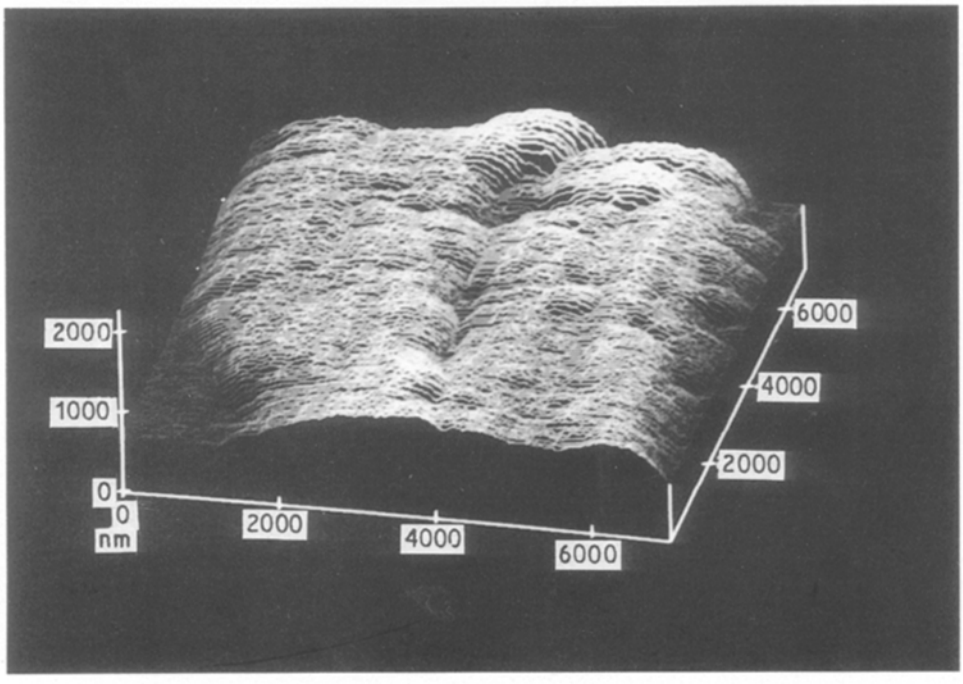

Figure 10 Portion of protruding conic marking. Direction of crack travel: top to bottom of picture (STM fractograph).

the secondary cracks in the mirror region are initiated at these impurities instead of at regions of decohesion between craze and matrix. The conic markings appear to be generated when the main crack overtakes these secondary cracks. The channels surrounding the particles at the foci of conic markings can be attributed to decohesion between the particle and the polymer matrix.

Acknowledgements

The authors acknowledge the support of the Department of Mechanical Engineering and Materials Science, Duke University, for this study. The STM facilities were provided by the Duke University Surface Science Center through a grant by AT & T.

References

1. D. HULL, in "Deformation and Fracture of High Polymers" (Plenum, New York, 1973) p. 171.
2. N. VERHEULPEN-HEYMANS, *Polymer* **20** (1979) 356.
3. J. G. WILLIAMS and G. P. MARSHALL, "Deformation and Fracture of High Polymers" (Plenum, New York, 1973) p. 557.
4. R. J. MORGAN and J. O'NEAL, *Polym. Engng Sci.* **18** (1978) 1081.
5. E. J. KRAMER and E. W. HART, *Polymer* **25** (1984) 1667.
6. W. G. KNAUSS, *Appl. Mech. Rev.* **26** (1973) 1.
7. R. P. KAMBOUR and R. E. BARKER, *J. Polym. Sci. A2* **4** (1966) 359.
8. R. N. HAWARD, B. M. MURPHY and E. F. T. WHITE, *ibid.* **9** (1971) 801.
9. R. P. KAMBOUR, *J. Polym. Sci. Macromol. Rev.* **7** (1973) 1.
10. D. G. LEGRAND, *J. Appl. Polym. Sci.* **13** (1969) 2129.
11. C. M. AGRAWAL and G. W. PEARSALL, *J. Mater. Sci.* **26** (1991) 1919–1930.
12. D. HULL and T. W. OWEN, *J. Polym. Sci. Polym. Phys. Ed.* **11** (1973) 2039.
13. R. J. MORGAN and J. E. O'NEAL, *Polymer* **20** (1979) 375.
14. *Idem., J. Polym. Sci. Polym. Phys. Ed.* **14** (1976) 1053.
15. G. H. JACOBY, "Electron Microfractography", ASTM STP 453 (American Society for Testing and Materials, Philadelphia, PA, 1969) p. 147.
16. R. RAVETTI, W. W. GERBERICH and T. E. HUTCHINSON, *J. Mater. Sci.* **10** (1975) 1441.
17. A. M. DONALD, T. CHAN and E. J. KRAMER, *ibid.* **16** (1981) 669.
18. P. BEAHAN, M. BEVIS and D. HULL, *ibid.* **8** (1972) 162.
19. L. H. LEE, J. F. MANDELL and F. J. McGARRY, *Polym. Engng Sci.* **27** (1987) 1128.
20. J. MURRAY and D. HULL, *Polymer* **10** (1969) 451.
21. *Idem., J. Polym. Sci. A2* **8** (1970) 583.
22. G. BINNIG and H. ROHRER, *Helv. Phys. Acta* **55** (1983) 726.
23. P. K. HANSMA and J. TERSOFF, *J. Appl. Phys.* **61**(2) (1987) R1.
24. P. H. CUTLER, T. E. FEUCHTWANG and Y. KUK, *Mater. Forum* **10**(2) (1987) 84.
25. C. M. AGRAWAL and G. W. PEARSALL, in "Proceedings of the 14th International Symposium on Testing and Failure Analysis", Los Angeles, 1988 (ASM International, Metals Park, 1988) p. 405.
26. M. AMREIN, A. STASIAK, H. GROSS, E. STOLL and G. TRAVAGLINI, *Science* **240** (1988) 514.
27. P. J. BRYANT, H. S. KIM, Y. C. ZHENG and R. YANG, *Rev. Sci. Instrum.* **58** (1987) 1115.
28. E. H. ANDREWS, "Fracture in Polymers" (Aberdeen University Press, London, 1968) p. 182.

Received 30 January
and accepted 4 September 1990